Atomic geometry and STM simulations of a TiO$_2$(1 1 0) surface upon formation of an oxygen vacancy and a hydroxyl group

P Mutombo[1,3], A M Kiss[2], A Berkó[2] and V Cháb[1]

[1] Institute of Physics of the Academy of Sciences of the Czech Republic, Cukrovarnicka 10, 162 53 Prague, Czech Republic
[2] Institute of Surface Chemistry and Catalysis/Reaction Kinetics Research, Laboratory of the Hungarian Academy of Sciences, University of Szeged, PO Box 168, H6701 Szeged, Hungary

E-mail: mutombo@fzu.cz

Abstract
The atomic geometry of a TiO$_2$(1 1 0) surface upon creation of an oxygen defect site and formation of a hydroxyl group was investigated using 3×1, 2×2 supercells by spin polarized density functional theory calculations. It was found that both the removal of a bridging O atom and the formation of an OH group lead to distortion in the atomic positions of the neighboring atoms depending on the choice of the unit cell used in the calculations. The scanning tunneling microscopy (STM) simulations performed using the 2×2 unit cell suggest that both an oxygen vacancy and a hydroxyl group should be observed experimentally as a bright protrusion but of different shapes. The O vacancy exhibits a spherical shape whereas the OH group was elongated perpendicular to the [0 0 1] direction. In contrast, in the 3×1 supercell, the OH group appears as a bright spot while the oxygen defect looks darker. These findings clearly suggest that a proper geometry is necessary to reproduce experimental STM images of an oxygen vacancy and a hydroxyl group on a TiO$_2$(1 1 0) surface.

1. Introduction

Oxygen vacancies play a significant role in influencing the physical and chemical properties of metal oxide surfaces. They can bind molecules, form active sites for their bond-breaking or act as preferential adsorption sites for metallic nanoparticles such as Au, Ag and Pd [1–8]. These properties have an impact on the performance of materials used in technological applications such as photovoltaic devices, catalytic systems and gas sensors [1]. Rutile constitutes one of

---

[3] Author to whom any correspondence should be addressed.

the prototype systems for heterogeneous reactions in catalysis as a support material. Oxygen vacancies on a rutile surface can be created during surface preparation by thermal annealing, ion bombardment, irradiation with UV light or by removal of oxygen with the tip in scanning tunneling microscopy (STM) experiments. Upon oxygen removal, the extra charge left can be redistributed in all the neighboring atoms or can remain trapped at the vacancy site. Some theoretical works predicted that this excess of electrons is essentially delocalized [9–11], while others claim that it is localized at the 3d orbitals of the nearby Ti atoms [12–17]. Experimental findings suggest that oxygen vacancies correspond to bright spots (type A-defect) appearing in dark rows in empty states' STM images [18]. This point of view was disputed by Suzuki, who argued that the bright spots are due to the adsorption of hydrogen on top of a bridging oxygen atom [19]. Furthermore, Schaub *et al* have distinguished two kinds of bright protrusions [20]. They associated the extended ones with oxygen vacancies while the smaller ones were ascribed to hydroxyl (OH) groups adsorbed at the vacancy sites. These OH groups are supposed to come from the dissociation of water present in the UHV chamber. Wendt *et al* claim that oxygen vacancies should be observed as faint protrusions, less bright than those caused by the hydroxyl group [21]. It is worth noting that both these two latter STM works may represent an evolution of ideas since they come from the same group. Based on the above survey, it is not clear how to distinguish the features connected to the oxygen vacancy from those due to the presence of a hydroxyl group.

In this work, density functional theory (DFT) is applied for the calculation of the changes in the atomic geometry due to the presence of oxygen defects and hydroxyl groups on the $TiO_2(1\,1\,0)$ surface. The aim is to determine how these morphological properties depend on the arrangement of the oxygen vacancies and the OH group at the TiO_2 surface. This is done by considering the 3×1 and 2×2 supercells, in which the concentration of the vacancy and OH group corresponds to 1/3 and 1/4 ML (see below). In addition, we would like to theoretically simulate the STM images of a point defect and a hydroxyl at different bias voltages in order to see if we can distinguish them.

2. Computational details

The present calculations were performed within the spin density polarized DFT using the hybrid B3LYP functional [22] as implemented in the CRYSTAL06 code [23]. The choice of this exchange-correlation functional was due to its ability to describe very well the localized states appearing in the band gap of insulators when oxygen vacancies are created or an OH group is formed [16, 17]. The Kohn–Sham orbitals are expanded as Gaussian-type functions. We used all electron basis sets for Ti 86-411d41,O 8-411d1 and H 3-11p1. Supercells of different sizes, i.e. 3×1 and 2×2, were used in order to determine the effect of the choice of the unit cell. All unit cells comprised nine atomic layers equivalent to three TiO_2 layers (figure 1). Previous periodic calculations have shown that this is a good approximation of the rutile surface [24]. All the layers, except the central TiO_2 one, were relaxed during the geometry optimization process. In CRYSTAL06, the optimization convergence is checked on the root-mean-square and the absolute value of the largest component of both the gradients and the estimated displacements. The optimizations of the geometry were done using the Berny algorithm until the maximum gradients and displacements were below 0.00045 and 0.0018 a.u., respectively. Nine and four k-points were used for the integration in the Brillouin zone for 3×1 and 2×2, respectively. To create an oxygen vacancy, one bridging oxygen atom per each side of the slab has been removed. The formation of a hydroxyl group was simulated by placing one single H atom (per each side of the slab) on top of a bridging oxygen atom. The simulation of the STM images was done following the Tersoff–Hamann approximation, where
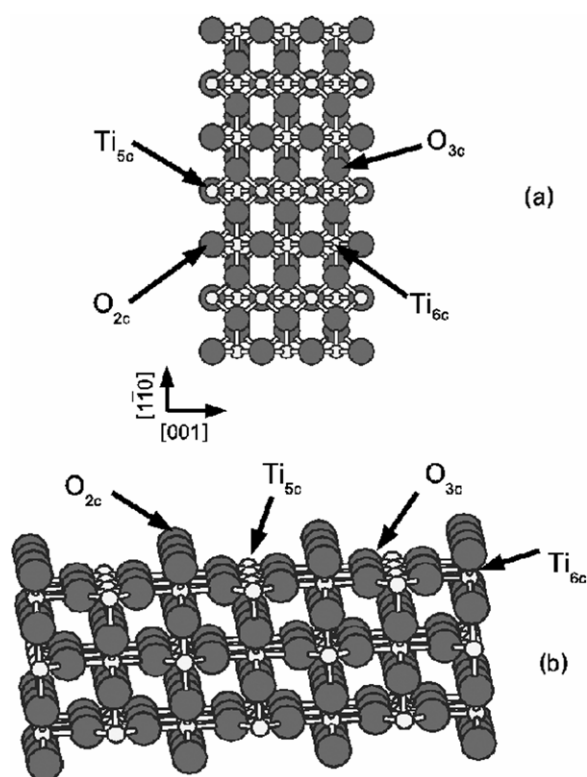
Figure 1. Top and side views of the TiO$_2$(1 1 0)-1 × 1 surface showing the different types of atoms: O$_{2c}$—bridging oxygen, Ti$_{6c}$—sixfold coordinated Ti atom, Ti$_{5c}$—fivefold coordinated Ti atom, O$_{3c}$—threefold coordinated in plane oxygen atom. White and dark balls indicate Ti and O atoms, respectively.

the tunneling current is proportional to the local density of states within a given bias voltage around the Fermi energy [25].

3. Results and discussions

Figure 1 displays top and side views of the TiO$_2$(1 1 0) surface. We can distinguish the following types of atoms: the bridging oxygen (O$_{2c}$), the sixfold (Ti$_{6c}$) and fivefold (Ti$_{5c}$) coordinated Ti cations and the threefold coordinated in plane oxygen atom (O$_{3c}$). The unit cells used in the calculations are depicted in figures 2(*a*) and (*b*). Before discussing the simulated STM images, first the structural changes appearing at the TiO$_2$ surface after the formation of an oxygen vacancy or an OH group will be considered. All atomic displacements reported in this paper are related to the calculated positions of the atoms in the relaxed TiO$_2$(1 1 0). On the clean relaxed TiO$_2$(1 1 0)-1 × 1, the O$_{2c}$ and the Ti$_{5c}$ atoms move downwards by 0.08 and 0.13 Å, whereas the O$_{3c}$ and Ti$_{6c}$ atoms rise up by 0.14 Å. These atomic displacements are related to their bulk terminated atomic positions. Some of the previous theoretical results indicated a very small displacement of the bridging oxygen atoms by about −0.02 Å [26, 27] and −0.06 Å [28]. The experiments showed a downward displacement by 0.27 Å [29] and 0.10 Å [30]. Our own previous DFT-LDA results indicated that the O$_{2c}$ and the Ti$_{5c}$ atoms
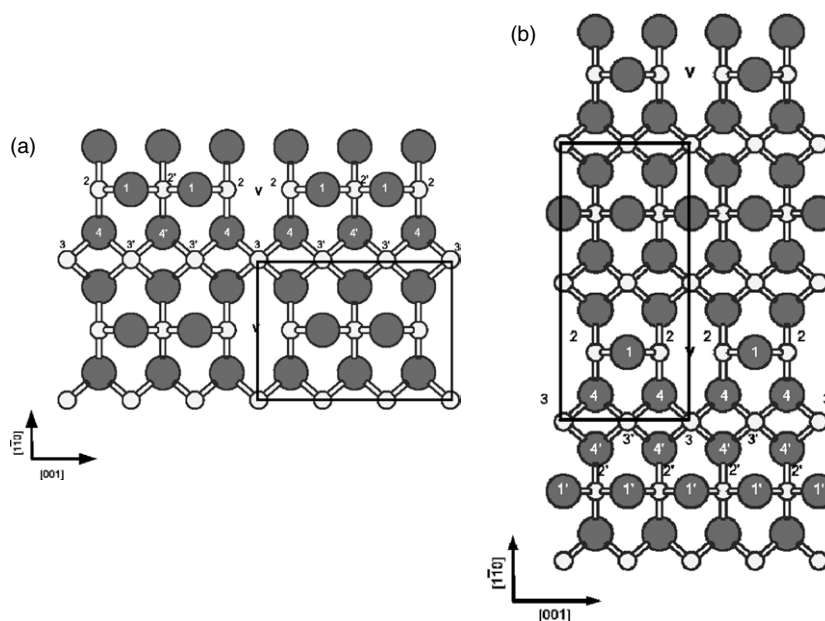
3

Figure 2. Schematic drawings of 3×1 and 2×2 unit cells are indicated in (*a*) and (*b*), respectively. 'V' represents an oxygen vacancy or an 'OH' group in the case of hydrogen adsorption on top of a bridging oxygen. The 1(1'), 2(2'), 3(3'), 4(4') denote the O_{2c}, Ti_{6c}, Ti_{5c} and O_{3c} atoms, respectively. Atoms '2' and '3' are not really sixfold and fivefold coordinated upon vacancy creation. The index '*'* refers to atoms distant from the vacancy (OH group). White and dark balls indicate Ti and O atoms, respectively.

move down by 0.12 Å and 0.16 Å, while the O_{3c} and Ti_{6c} atoms rise up by 0.12 Å and 0.08 Å, respectively [31]. As for Ti_{6c}, the experiments indicated an upwards movement by 0.12 Å [29] and 0.25 Å [30], while the other theoretical calculations reported 0.19 Å [26], 0.23 Å [27] and 0.13 Å [28], respectively. Both theory and experiments agree with the downward relaxation of the Ti_{5c} atom. There is also some discrepancy among the experimental findings and theory for the position of the O_{3c} atoms. The disagreement between the different theoretical results is probably caused by the difficulty in finding the global absolute minimum energy of such a flat surface and by the different computational parameters used in the calculations. On the other hand, the differences in the experimental results may be due to different experimental conditions.

Figures 3(*a*) and (*b*) exhibit the atomic geometry of a $TiO_2(1\,1\,0)$-1×1 surface upon creation of an oxygen vacancy for different unit cells. First, we need to point out that Ti_{6c} and Ti_{5c} atoms closer to the vacancy become fivefold (Ti_{65c}) and fourfold (Ti_{54c}) coordinated atoms, respectively, upon the removal of a bridge oxygen atom. It can be seen that all atoms of the topmost layers have been affected by the creation of a vacancy. There is a significant upward displacement of the remaining O_{2c} atoms with respect to their positions in a relaxed TiO_2 $(1\,1\,0)$ for the 3×1 unit cell. They relax upwards by 0.11 Å. In contrast, this upward displacement is very small (0.02 Å) in the 2×2 supercell. Ti_{65c} atoms (type '2') move inwards by 0.20 (0.14) Å for the $3 \times 1(2 \times 2)$ unit cells, compared with Ti_{6c} atoms (type 2') which relaxed outwards by 0.24 (0.02) Å. This means that the presence of a vacancy affects more Ti_{65c} and Ti_{6c} atoms in the 3×1 unit cell than in the 2×2 one. The Ti_{5c} cations and the O_{3c} atoms rise up in both the supercells; however, the magnitude of their relaxation depends on their
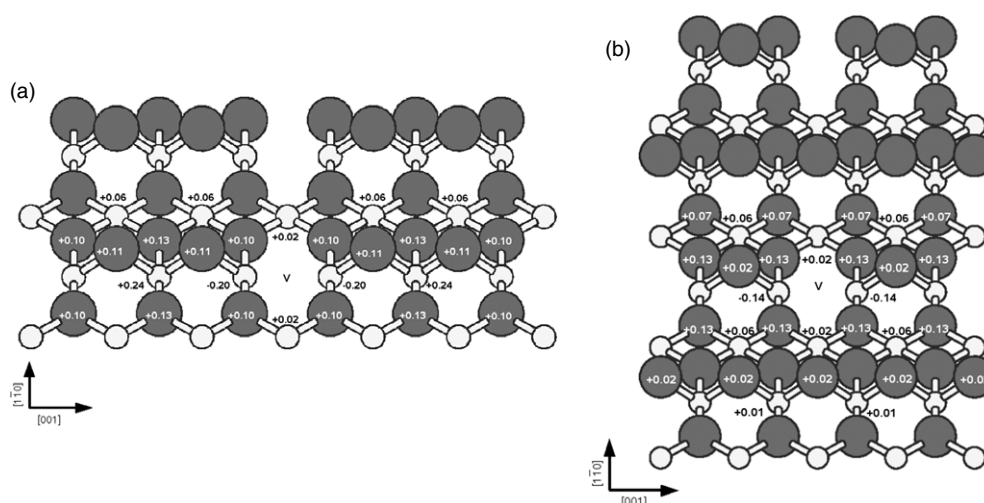
Figure 3. Atomic displacements in angstrom (Å) of the topmost layers upon creation of a vacancy by removing a bridging oxygen. All displacements refer to the positions of the atoms in the relaxed TiO_2 (1 1 0)-1 $\times$ 1 surface. Figures (*a*) and (*b*) show structural geometry in the 3 $\times$ 1 and 2 $\times$ 2 unit cells, respectively. White and dark balls indicate Ti and O atoms.

distance to the vacancy. The Ti_{5c} atoms positioned far from the vacancy are affected strongly. The O_{3c} atoms nearer the vacancy move up by 0.10 (0.13) Å in the 3 $\times$ 1(2 $\times$ 2) unit cells while those farther shift up by 0.13 (0.07) Å, respectively. The above results differ from the earlier reports of Ramamoorthy *et al* [12] and Mackrodt *et al* [14] who found inward relaxations of 0.02 Å [12], 0.05 Å [14] and 0.10 Å [12], 0.13 Å [14] for Ti_{65c} and Ti_{54c} coordinated atoms and an outward relaxation of 0.35 Å [12] and 0.39 Å [14] for surface oxygen atoms.

Thus, it can be said that the removal of an oxygen atom induced strong distortion in the atomic geometry depending on the choice of the unit cell. Vacancies tend to repulse themselves on a rutile surface [32]. Consequently, their spatial configuration at the surface is determinant for the final geometry of the TiO_2(1 1 0) surface.

Upon adsorption of hydrogen at the bridging oxygen, the oxygen of the OH group relaxed upwards by 0.12 (0.14) Å in the 3 $\times$ 1(2 $\times$ 2) supercells. The other O_{2c} atoms rise up by 0.07 Å in the 3 $\times$ 1 unit cell while their positions are almost unchanged in the 2 $\times$ 2 unit cell (figure 4(*a*)). However, the O_{2c} atoms in the same oxygen row as the OH group rise up slightly by 0.03 Å. The Ti_{6c} cations closer to the OH group shift down by 0.09 (0.05) Å for the 3 $\times$ 1 (2 $\times$ 2) unit cells. In contrast, those farther from it move up by 0.09 Å in the 3 $\times$ 1 unit cell only. Their positions remain almost unaffected in the 2 $\times$ 2 cell. The formation of a hydroxyl group does not affect in the same way the Ti_{5c} and O_{3c} atoms in the 3 $\times$ 1 unit cell. Some Ti_{5c} cations and O_{3c} atoms rise up by 0.04 Å and 0.06 Å, respectively, while others remain at their initial positions. Moreover, we found that the Ti_{5c} cations keep their initial geometry in the 2 $\times$ 2 unit cell whereas the O_{3c} atoms rise slightly by 0.03 Å. In brief, the formation of an OH group leads to a strong structural distortion in the 3 $\times$ 1 supercell compared with the 2 $\times$ 2 one. H atom bonds to the oxygen atom, whose lengths are 0.971 Å (3 $\times$ 1) and 0.97 Å (2 $\times$ 2). These values are very close to the experimental value of 0.96 Å in a free water molecule suggesting the presence of a polar covalent bond [33].

Figure 5 displays the total density of states of the reduced ((*a*), (*c*)) and hydroxylated ((*b*), (*d*)) surfaces. One sees localized states (indicated by arrows) in the band gap. These
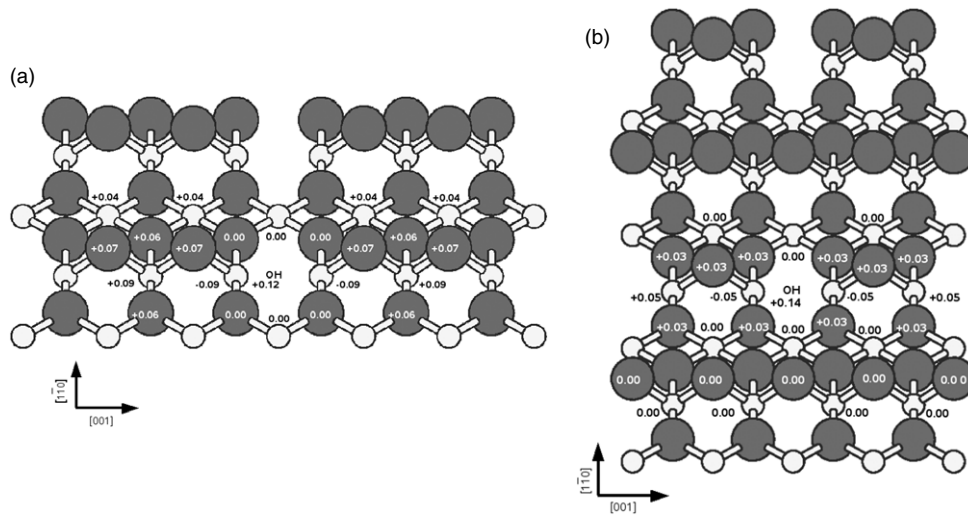
Figure 4. Atomic displacements in angstrom (Å) of the topmost layers upon adsorption of hydrogen on top of a bridging oxygen for different unit cells. All displacements refer to the positions of the atoms in the relaxed TiO_2 (1 1 0)-1 × 1 surface. Figures (*a*) and (*b*) show structural geometry in the 3 × 1 and 2 × 2 unit cells, respectively. White and dark balls indicate Ti and O atoms.
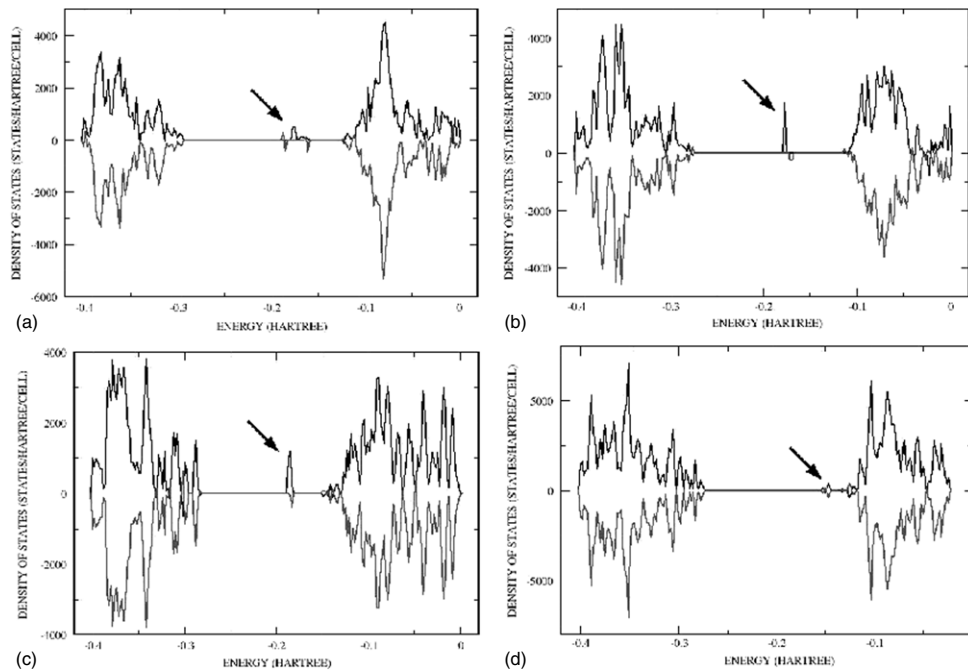

Figure 5. Total density of states for the reduced (*a*), (*c*) and hydroxylated surfaces (*b*), (*d*). Black arrows show the localized states in the band gap. Spin up and down are shown.

states arise from the electron trapping in the 3d states of the titanium atoms near the oxygen vacancy or the hydroxyl group [34]. Empty states' STM maps simulated on clean, reduced and hydroxylated surfaces are shown in figures 6, 7 and 8. We report only maps at 1.7 eV since no dependence on the applied bias voltage was found. The map for the clean surface
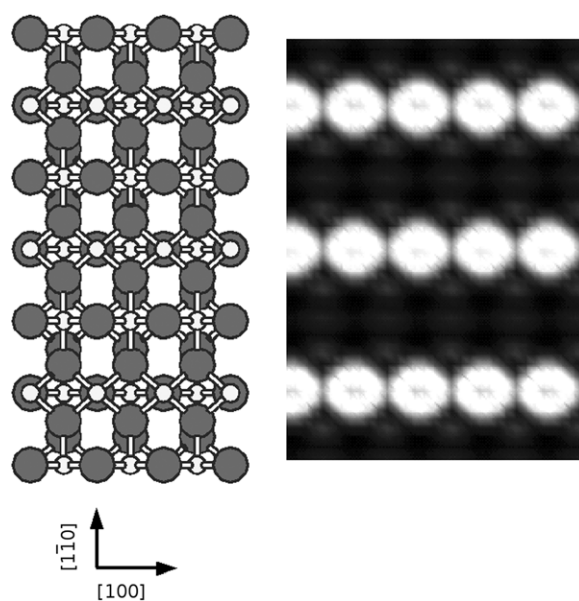
$[1\bar{1}0]$

$[100]$

Figure 6. Simulated constant-height (2.5 Å) empty states' images of a clean surface at 1.9 V. The height is taken with respect to the topmost bridging oxygen atoms. Bright spots correspond to titanium rows. An atomistic model of the unit cell is shown together with the simulated STM image.
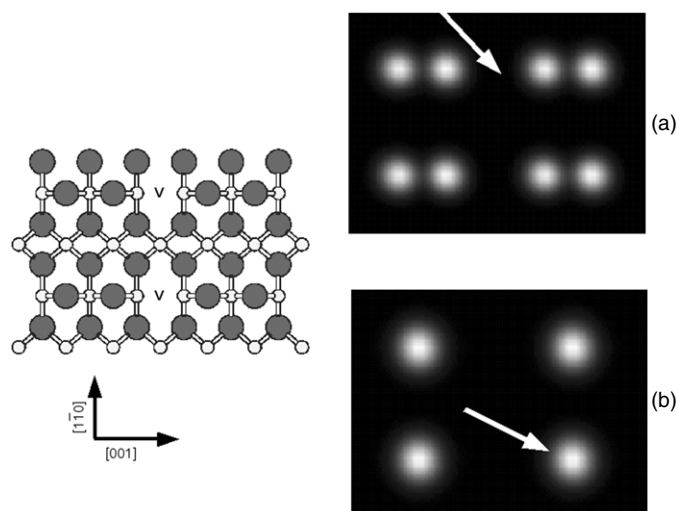

(a)

(b)

$[1\bar{1}0]$

$[001]$

Figure 7. Simulated constant-height (3 Å) empty states' images at 1.7 eV for the 3 × 1 unit cell. Figures (*a*) and (*b*) refer to the reduced and hydroxylated surfaces, respectively. The height is taken with respect to the topmost bridging oxygen atoms. A white arrow shows the oxygen vacancy (OH group) in (*a*) and (*b*), respectively . An atomistic model of the unit cell is shown together with the simulated STM images.

shows the Ti rows like bright protrusions. This means that the electrons are tunneling from the tip into Ti_{5c} empty states rather than into the topmost bridging oxygen atoms. This agrees with experimental results. STM maps simulated for the 3 × 1 unit cell show bridging oxygen atoms as bright spots (figure 7(*a*)) whereas the oxygen defect appears as dark. This contrast
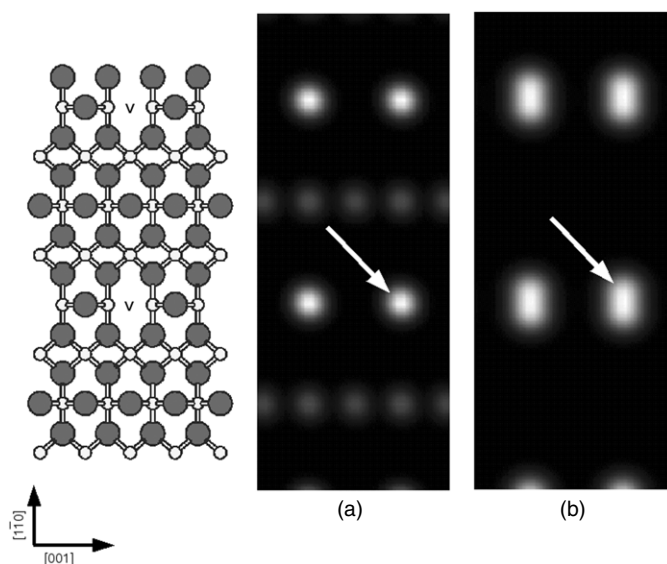
Figure 8. Simulated constant-height (3 Å) empty states' images at 1.7 eV. The height is taken with respect to the topmost bridging oxygen atoms. A white arrow shows the oxygen vacancy (OH group). Gray spots in (*a*) correspond to the position of bridging oxygen atoms of the next row. An atomistic model of the unit cell is shown together with the simulated STM images.

reversal is in contradiction to the experimental findings which display a vacancy as a bright protrusion. We think that this surprising situation can be connected to the atomic geometry of the 3×1 unit which is different from the one actually present at the surface. We found that the distance between the two remaining O_{2c} atoms across the vacancy is actually 5.77 Å instead of the usual value of 5.9 Å. For comparison, the same distance in the 2×2 unit equals 5.9 Å. A shorter distance indicates that both O_{2c} atoms are attracted by the O vacancy. Such lattice distortion may induce a change in the local density of states at the vacancy site. In contrast to the 3×1 supercell, the oxygen vacancies appear as bright spots of spherical shape (figure 8(*a*)) in the 2×2 unit cell. They have spherical shape. The bridging oxygen atoms of the next row are imaged as gray spots. Under normal conditions they are not seen in experimental STM images. Our results suggest that if there is a local 2×2 structure of a vacancy, the O_{2c} atoms of the next oxygen row can be imaged as gray spots. Simulated STM images of hydroxylated surfaces (figures 7(*b*) and 8(*b*)) strongly resemble the so-called type-A defect [18]. This means that this kind of defect is likely due to the OH group than the oxygen vacancy.

These results suggest that a good geometry is necessary to reproduce some features of the experimental findings. Since the STM images are rather dominated by the electronic effects than by the topographic ones, consequently the appearance of the observed features depend on the charge rearrangement at the surface. The latter is in turn connected to the atomic arrangement at the surface. Thus, the choice of the unit cell in the theoretical calculations is a crucial parameter in order to obtain reliable results.

4. Conclusion

Spin polarized DFT calculations presented in this work suggest that the creation of an oxygen vacancy and the adsorption of an H atom on a bridging oxygen site induce a strong distortion in

the atomic geometry of the surrounding atoms on the $TiO_2(1\,1\,0)$-1×1 surface. The distortion depends on the defect arrangement at the surface and thus on the choice of the supercell of the $TiO_2(1\,1\,0)$ unit cell used in the calculations. Empty state STM images simulated for a 2×2 unit cell suggest that an oxygen vacancy should appear as a bright spherical spot in contrast to the OH group which should have an elongated shape. On a 3×1 supercell, the oxygen vacancy should appear darker while the OH should be observed as a bright spot. These results suggest that the oxygen vacancy and the hydroxyl group are experimentally distinguishable.

Acknowledgments

References

[1] Diebold U 2003 *Surf. Sci. Rep.* **48** 53
[2] Bikondoa O, Pang Chi L, Ithnin R, Muryn C A, Onishi H and Thornton G 2006 *Nature Mater.* **5** 189
[3] Henderson M A, Epling W S, Peden C H F and Perkins C L 2003 *J. Phys. Chem.* B **107** 504
[4] Giordano L, Goniakowski J and Pacchioni G 2001 *Phys. Rev.* B **64** 075417
[5] Tong X, Benz L, Chrétien S, Kemper P, Kolmakov A, Metiu H, Bowers M T and Buratto S K 2005 *J. Chem. Phys.* **123** 204701
[6] Wahlström E, Lopez N, Schaub R, Thostrup P, Rønnau A, Africh C, Laegsgaard E, Nørskov J K and Besenbacher F 2003 *Phys. Rev. Lett.* **90** 026101
[7] Jak M J J, Konstapel C, Van Kreuningen A, Chrost J, Verhoeven J and Frenken J W M 2001 *Surf. Sci.* **474** 28
[8] Kiss A M, Svec M and Berkó A 2006 *Surf. Sci.* **600** 3352
[9] Vijay A, Mills G and Metiu H 2003 *J. Chem. Phys.* **118** 6536
[10] Paxton A T and Thiên-Nga L 1998 *Phys. Rev.* B **57** 1579
[11] Pillay D and Hwang G S 2005 *Phys. Rev.* B **72** 205422
[12] Ramamoorthy M, King-Smith R D and Vanderbilt D 1994 *Phys. Rev.* B **49** 7709
[13] Burton J, Bullet D W, Oliver P M and Parker S C 1995 *Surf. Sci.* **336** 166
[14] Mackrodt W C, Simson E A and Harrison N M 1997 *Surf. Sci.* **384** 192
[15] Lindan P J D, Harrison N M, Gillan M J and White J A 1997 *Phys. Rev.* B **55** 15919
[16] Bredow T and Pacchioni G 2002 *Chem. Phys. Lett.* **355** 417
[17] Di Valentin C and Pacchioni G 2006 *Phys. Rev. Lett.* **97** 166803
[18] Diebold U, Lehman J, Mahmoud T, Kuhn M, Leonardelli G, Hebenstreit W, Schmid M and Varga P 1998 *Surf. Sci.* **411** 137
[19] Suzuki S, Fukui K-i, Onishi H and Iwasawa Y 2000 *Phys. Rev. Lett.* **84** 2156
[20] Schaub R, Thostrup P, Lopez N, Lægsgaard E, Stensgaard I, Nørskov J K and Besenbacher F 2001 *Phys. Rev. Lett.* **87** 266104/1
[21] Wendt S *et al* 2005 *Surf. Sci.* **598** 226
[22] Lee C, Yang W and Parr R G 1988 *Phys. Rev.* B **37** 785
[23] Dovesi R *et al* 2006 *CRYSTAL06 User's Manual* (Torino: University of Torino)
[24] Sambrano J R, Nobrega G F, Taft C A, Andres J and Beltran A 2005 *Surf. Sci.* **580** 71
[25] Tersoff J and Hamann D R 1985 *Phys. Rev.* B **31** 805
[26] Wang Y and Hwang G S 2003 *Surf. Sci.* **542** 72
[27] Bates S P, Kresse G and Gillan M J 1997 *Surf. Sci.* **385** 386
[28] Yang Z, Wu R and Goodman D W 2000 *Phys. Rev.* B **61** 14066
[29] Charlton G *et al* 1997 *Phys. Rev. Lett.* **78** 495
[30] Lindsay R, Wander A, Ernst A, Montanari B, Thornton G and Harrison N M 2005 *Phys. Rev. Lett.* **94** 246102
[31] Mutombo P, Kiss A M, Berkó A and Cháb V 2006 *Nanotechnology* **17** 4112
[32] Rasmussen M D, Molina L M and Hammer B 2004 *J. Chem. Phys.* **120** 988
[33] Sim F, St-Amant A, Papai I and Salahub D R 1992 *J. Am. Chem. Soc.* **114** 4391
[34] Kurtz R L, Stock-Bauer R, Madey T E, Román E and De Segovia J L 1989 *Surf. Sci.* **218** 178